Crimson Publishers
Wings to the Research

Mini Review

First Principle Investigations of $La_{0.25}Sm_{0.75}O_{1.5}$ Structure: Spin Polarized, LDA+U Calculations

Alsulaim GM[1], El-Amin AA[2]* and Khalafalla MAH[3]

[1]The Eastern Province-Al-Ahsa-King Faisal University, Saudi Arabia

[2]Physical department, Faculty of Science, Aswan University, Egypt

[3]Faculty of Science, Yanbu, Taibah University, Saudi Arabia

ISSN: 2578-0255

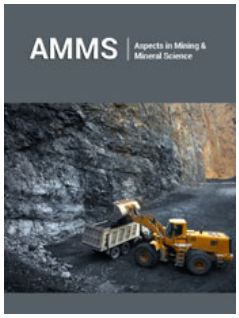

***Corresponding author:** A A El-Amin, Physical department, Faculty of Science, Aswan University, Egypt

Submission: January 25, 2023

Published: February 08, 2023

Volume 10 - Issue 5

How to cite this article: Alsulaim GM, El-Amin AA*, Khalafalla MAH. First Principle Investigations of $La_{0.25}Sm_{0.75}O_{1.5}$ Structure: Spin Polarized, LDA+U Calculations. Aspects Min Miner Sci. 10(5). AMMS. 000748. 2023.
DOI: 10.31031/AMMS.2023.10.000748

Summary

The authors report on the spin polarized first principle investigations of a $Sm_{0.75}La_{0.25}O_{1.5}$ structure under the framework of Hubbard potential correction (LDA+U correction) for the potential between the localized electrons in the f- and d-orbital. The lattice parameters of the structure were extracted from Rietveld refinement of the X-ray diffraction pattern which revealed that the structure was monoclinic with C 12/m1 space group symmetry. The information about the structure's symmetry allowed us to construct the random supercell, $Sm_9La_3O_{18}$, for the density functional first principle calculation. The $Sm_9La_3O_{18}$ has been generated with software for efficient stochastic generation of special quasi random structures. The Calculated Density of States (DOS) with LDA+U correction showed that the structure was non-metallic in contrast to the calculation without LDA+U correction which gave rise to a metallic structure. Similar LDA+U calculation on Sm_6O_9 has also revealed non-metallic structure in an agreement with the experiment on monoclinic Sm_2O_3. The distribution of the DOS among the spin-up and spin-down electrons in the f and d orbitals suggest that the variation in the structure composition (percentage of Sm and La) and doping with another elements may give rise to an interesting controllability in the structure magnetization.

Keywords: Density functional calculation; Spin polarized first principle; LDA+U correction; Rare earth elements

Introduction

Sharma et al. [1] reported about first-ever ab-initio calculation in Sm_2O_3, wherein they calculated the density of states and other computational parameters compatible with available experimental data. On the other hand, Elamin et al. [2] has demonstrated the importance of their novel $LaSmO_2$ structure in hydrogen fuel cells applications. These works [1,2] clearly indicate that theoretical and computational analysis in rare earth compounds comprising La and Sm are highly important and will have significant impact on fuel cell as well as solar cell applications (e.g. [3]). This has motivated us to calculate the spin-polarized density of states of monoclinic $Sm_{0.75}La_{0.25}O_{1.5}$ (hereafter referred to simply as SmLaO) under the scheme of density functional theory [4-7] while correcting the Coulomb potential for the localized electrons in the f- and d-orbital of Sm and La. Such a correction is well known as LDA+U [8], where U refers to the Hubbard potential [9] employed in this correction. Our results show that the structure is non-metallic, in an agreement with Lal et al. [10] experiment in monoclinic Sm_2O_3.

Rietveld Refinement of X-Ray Pattern from the Synthesized $Sm_{0.25}La_{0.75}O_{1.5}$ Structure

The SmLaO was prepared following the same recipe described in Ref# [2] but with deferent La_2O_3 and Sm_2O_3 compositions. We used the MAUD (Material Analysis Using Diffraction [11]) code to refine the X-ray pattern for SmLaO which is shown as blue squares in Figure 1a. The black solid line in Figure 1a is the Rietveld refinement [12] of the X-ray data. The best fit was accomplished with space group=C12/m (monoclinic symmetry) where the occupancies of

the 4i Wyckoff positions were, respectively, 0.23, 0.77 and 1 for La (3 atoms), Sm (3 atoms) and O (4 atoms) and the 2b Wyckoff occupancy was 1 for O (1 atom). These occupancies were adopted from the synthesis information. The refined lattice parameters were a=14.3945 A, b=3.6835 A, c=8.9795 A, alpha= gamma=900, and beta=100.680. The Rietveld refinement R-factor and goodness-of-fit were 0.251 and 0.341, respectively, and the difference between the experiment and fitting line was almost flat as illustrated in the bottom rectangular panel of Figure 1a. However, to simplify the analysis we approximate the Sm and La occupancies as 0.75 and 0.25, respectively. In this case, the experimental structure can be viewed as a periodically repeated unit cell consisting of 30 atoms, i.e. $Sm_9La_3O_{18}$. Such a periodic unit cell is called the supercell in the terminology of first-principle calculation [7]. Our choice of the 30 atoms supercell was based on the compatibility of this cell size with the available computational resources. However, the accuracy of the calculation improves for large supercells but this will be at the expense of the higher computational demand. However, our supercell cell size is large enough to convey useful information and for comparison with experimental results.

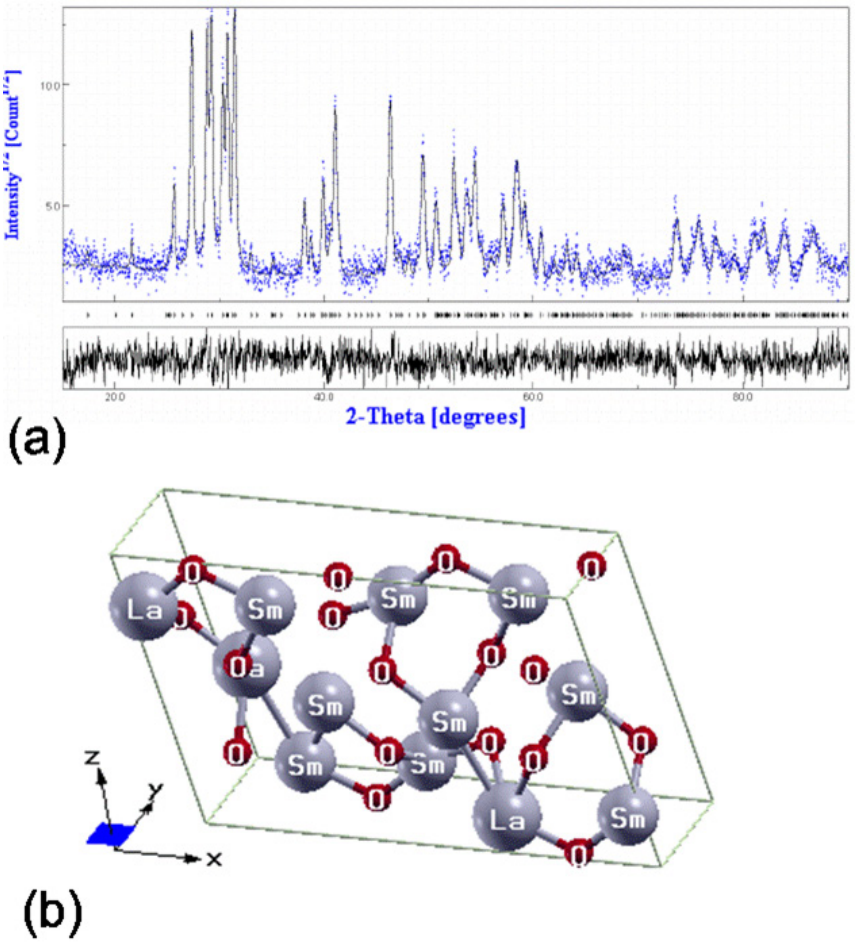

Figure 1: (a) X-ray pattern (blue squares) for our synthesized $Sm_{0.77}La_{0.23}O_{1.5}$ and the retvield refinement (black line) of the X-ray pattern using MAUD program (see text). (b) The structure of the supercell $Sm_9La_3O_{18}$ used in the first principle calculation.

First-Principle Calculation of SmLaO Band Structure: Computational Method

Special quasirandom structure method: generation of $Sm_9La_3O_{18}$

The Structure Method (SQS) code called "mcsqs" [13] was employed to generate the random $Sm_9La_3O_{18}$ supercell structure. The essence of this code is that it generates the best periodic supercell approximations to the true disordered state for a given number of atoms per supercell. This greatly reduces the huge computational demand pertinent to random structure calculation which requires huge number of atoms per supercell. The code uses two input files: one (called rndstr.in) containing the lattice parameters and atomic positions and another cluster configuration sites which provides information about the lattice Nearest-Neighbor (NN) ranges. The cluster file was generated with the "corrdump" code which is part of the open-source Alloy-Theoretic-Automated Toolkit [14]. The NN ranges for pairs, triplets and quadruplets were 6 Å and 5 Å and 5 Å, respectively. Here it is worth mentioning again that the atomic composition x=0.25 used in rndstr.in for La is slightly different from the experimental 0.23. However, we expect that with this slight discrepancy the Density of States (DOS) will still be reliable

and instructive. Additionally, the choice of x=0.25 facilitates the generation of $Sm_{0.75}La_{0.25}O_{1.5}$ SQS with reasonable size containing 30 atoms, i.e. $Sm_9La_3O_{18}$. The generated SQS structure with 30 atoms is shown in Figure 1b. All the generated supercell structures were carefully relaxed to minimize the forces between atoms to ~ 0.05eV/Å. The force relaxation process was implemented using the first-principle density-functional (DFT) software package called the QUANTUM ESPRESSO (QE) which is a modular and open-source software project for quantum simulations of materials [15]. The calculation method using QE will be discussed in the next section 3.2. For simplicity we have not performed structural relaxation of the lattice parameters.

Calculation of the density of states (DOS)

The QE software periodically expands the finite size supercell (Figure 1b) to mimic the infinitely large real material. Basically, the software uses plane waves basis sets and pseudopotentials [16] to represent the electron-ion interactions. The Generalized Gradient Approximation (GGA) pseudopotentials of Perdew–Burke–Ernzerhof (PBE) [6] were employed for the elements La, Sm and O. In particular we have used the accurate Projected Augmented Wave (PAW) pseudopotentials optimized by Topsakal et al. [17] for rare-earth elements including Sm and La. For oxygen element we have used a PAW pseudopotential similar to the ones that can be downloaded from the QE website [18]. The cutoff for the electron's kinetic energy (plane wave energy) was set at 680eV. The k-point mesh of 2 3 1 size was generated using the Monkhorst-Pack method [19] for the Brillouin zone integration. The convergence threshold for the self-consistent calculation of the total energy was 0.0014eV.

First-Principle Calculation: Results and Discussions

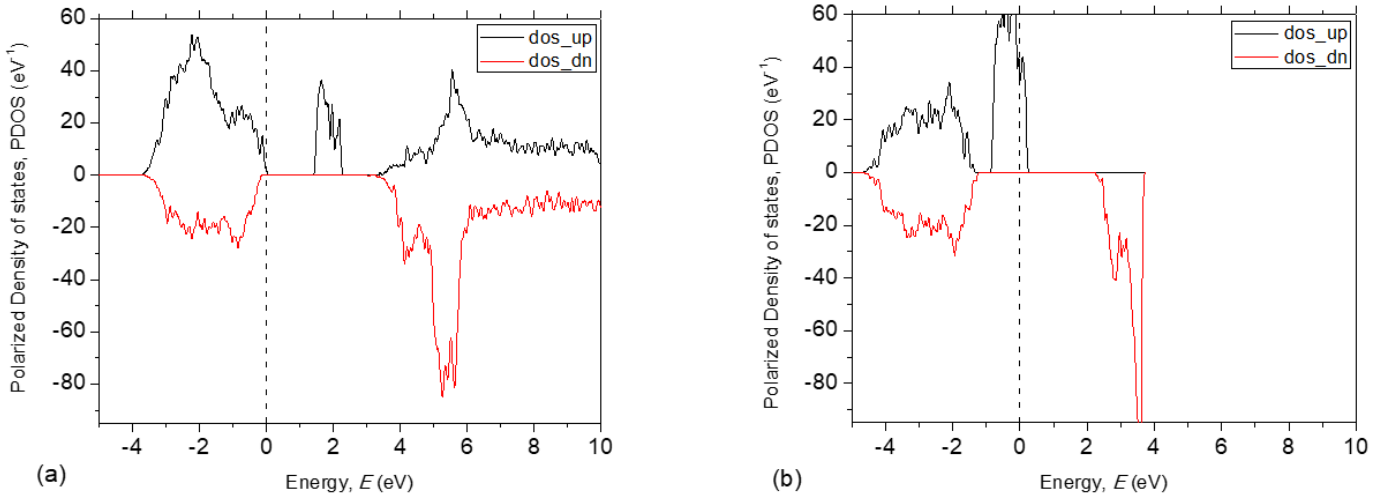

Figure 2: The spin polarized density of states calculated in $Sm_9La_3O_{18}$ (a) with LDA+U correction and (b) without LDA+U correction.

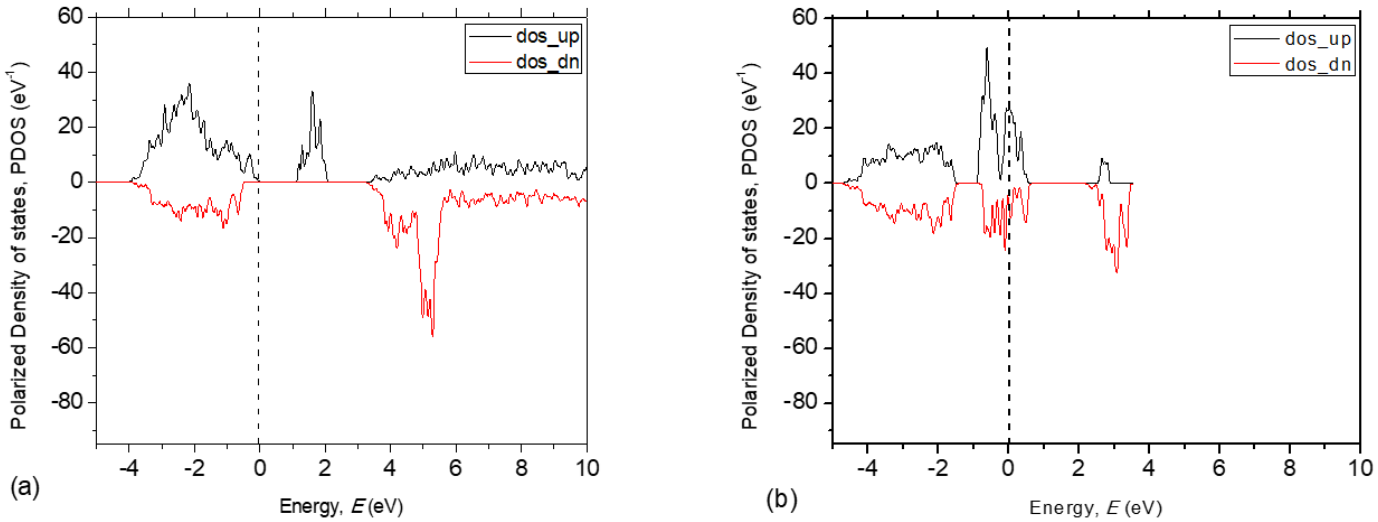

Figure 3: The spin polarized density of states calculated in Sm_2O_3 (a) with LDA+U correction and (b) without LDA+U correction.

Figures 2a & 2b show the calculated polarized density of states (PDOS), respectively, obtained with and without the LDA+U correction. The spin-up (dos_up) and spin-down (dos_dn) PDOS are indicated by the black and red lines in Figure 2. The Hubbard potentials were 3.3eV and 9eV for Sm (f-orbital) and La (d-orbital), respectively. These values were optimized by Topsakal et al. [17]. The Fermi level (dashed line, Figure 2) at 0eV designates the topmost occupied level. Clearly, the Fermi level is at the top of the valence band in Figure 2a and is inside the spin-up conduction band in Figure 2b. This indicates that the calculation without LDA+U correction predicts a metallic $Sm_{12}La_3O_{18}$, while the LDA+U predicts a non-metallic structure. We have also performed similar calculations as that in (Figure 2) but for Sm_2O_3. The results are shown in Figure 3. Again, judging from the location of the Fermi level (dashed line, Figure 3), the LDA+U predicts a non-metallic Sm_2O_3 in an agreement with Lal et al. [10] experiment on monoclinic Sm_2O_3 but in contrast to the non-LDA+U result in Figure 3b. Since (Figures 2 & 3) have almost similar PDOS patterns, we conclude that our structure is also non-metallic. The observed increase in the PDOS in Figure 2 compared with that in Figure 3 is due to larger supercell for (Figure 2) (i.e., $Sm_9La_3O_{18}$) than that in Figure 3 (i.e., Sm_6O_9).

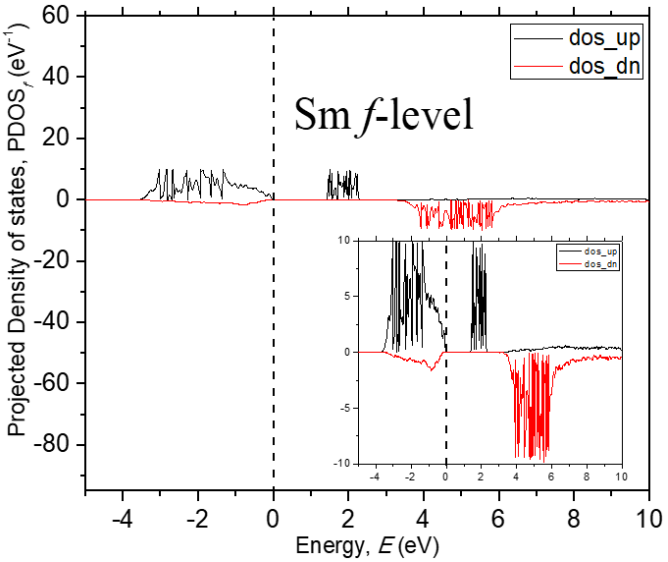

Figure 4: The projected spin polarized density of states on the Sm f-orbital calculated in $Sm_9La_3O_{18}$. (a) with LDA+U correction and (b) without LDA+U correction.

The projected density of states on the f-orbital ($PDOS_f$) and d-orbital ($PDOS_d$) for Sm and La, respectively, are shown in Figures 4 & 5 for the case of LDA+U correction. Clearly, the added trace of La gave rise to even distribution of $PDOS_d$ among the spin-up and spin-down electrons in the valence (below the Fermi level) and conduction bands. This is in contrast to the $PDOS_f$ distribution among spin-up electrons in the valence band and the spin-down electrons in the conduction band. These behaviors of $PDOS_d$ and $PDOS_f$ suggest that controllability of La and Sm composition may affect the structure magnetization. Such controllability on the magnetization may be enhanced by doping the material with another element. However, we will leave the detailed study of the effect of doping and composition variation on magnetization as well as on the mechanical and electrical properties for future work.

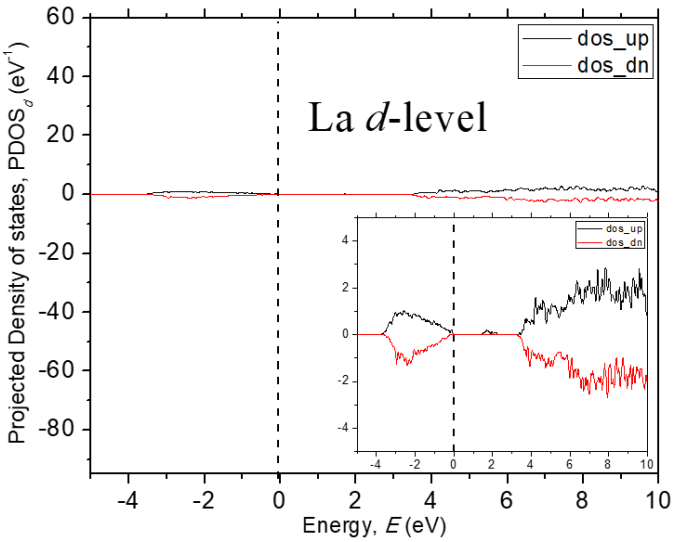

Figure 5: The projected spin polarized density of states on the La d-orbital calculated in $Sm_9La_3O_{18}$ (a) with LDA+U correction and (b) without LDA+U correction.

Conclusion

We have investigated the spin polarized first principle density of states in $Sm_{0.75}La_{0.25}O_{1.5}$ structure under the framework of Hubbard potential correction (LDA+U correction) for the potential between the localized electrons in the f- and d-orbital. The lattice parameters of the structure were extracted from Rietveld refinement of the X-ray diffraction pattern which revealed that the structure was monoclinic with C 12/m1 space group symmetry. The information about the structure's symmetry allowed us to construct the random supercell, $Sm_9La_3O_{18}$, (equivalent to $Sm_{0.75}La_{0.25}O_{1.5}$) for the density functional first principle calculation. The $Sm_9La_3O_{18}$ has been generated with "mcsqs" which is a software for efficient stochastic generation of special quasi random structures. The Calculated Density of States (DOS) with LDA+U correction showed that the structure was non-metallic in contrast to the calculation without LDA+U correction which gave rise to a metallic structure. Similar LDA+U calculation on Sm_6O_9 has also revealed non-metallic structure in an agreement with the experiment on monoclinic Sm_2O_3. The distribution of the DOS among the spin-up and spin-down electrons in the f and d orbitals suggest that the variation in the structure composition (percentage of Sm and La) and doping with other elements may give rise to an interesting controllability in the structure magnetization.

References

1. Sharma S, Heda NL, Suthar KK, Bhatt S, Sharma K, et al. (2015) Ab-initio calculations for electronic structure and momentum densities of samarium sesquioxide. Computational Materials Science 104: 205-211.

2. El-Amin AA, Othman AM (2016) Novel GO-$LaSmO_2$ nanocomposite as an effective electrode material for hydrogen fuel cells. JOM 68(4): 1209-1215.

3. Corma A, Atienzar P, Garcia H, Chane Ching JY (2004) Hierarchically mesostructured doped CeO_2 with potential for solar-cell use. Nature materials. 3(6): 394-397.

4. Parr RG (1980) Density functional theory of atoms and molecules. Horizons of Quantum Chemistry pp. 5-15.

5. Car R, Parrinello M (1985) Unified approach for molecular dynamics and density-functional theory. Physical Review Letters 55(22): 2471.

6. Perdew JP, Burke K, Ernzerhof M (1996) Generalized gradient approximation made simple. Physical Review Letters 77(18): 3865.

7. Sholl D, Steckel JA (2011) Density functional theory: A practical introduction. John Wiley & Sons, US.

8. Liechtenstein A, Anisimov V, Zaanen J (1995) Density-functional theory and strong interactions: Orbital ordering in Mott-Hubbard insulators. Physical Review B 52(8): R5467.

9. Anisimov VI, Zaanen J, Andersen OK (1991) Band theory and mott insulators: Hubbard U instead of stoner I. Physical Review B 44(3): 943.

10. Lal H, Gaur K (1988) Electrical conduction in non-metallic rare-earth solids. Journal of Materials Science 23(3): 919-923.

11. Lutterotti L, Matthies S, Wenk H (1999) MAUD (material analysis using diffraction): A user friendly Java program for Rietveld texture analysis and more. Proceeding of the twelfth international conference on textures of materials (ICOTOM-12). NRC Research Press Ottowa, Canada.

12. Thompson P, Cox D, Hastings J (1987) Rietveld refinement of debye–scherrer synchrotron X-ray data from Al_2O_3. Journal of Applied Crystallography 20(2): 79-83.

13. Van de Walle A, Tiwary P, Jong M, Olmsted DL, Asta M, et al. (2013) Efficient stochastic generation of special quasirandom structures. Calphad 42: 13-18.

14. Van de Walle A, Asta M, Ceder G (2002) The alloy theoretic automated toolkit: A user guide. Calphad 26(4): 539-553.

15. Giannozzi P, Baroni S, Bonini N, Calandra M, Car R, et al. (2009) QUANTUM ESPRESSO: A modular and open-source software project for quantum simulations of materials. Journal of Physics: Condensed Matter 21(39): 395502.

16. Pickett WE (1989) Pseudopotential methods in condensed matter applications. Computer Physics Reports 9(3): 115-197.

17. Topsakal M, Wentzcovitch R (2014) Accurate projected augmented wave (PAW) datasets for rare-earth elements (RE=La–Lu). Computational Materials Science 95: 263-270.

18. http://www.quantum-espresso.org/pseudopotentials/

19. Monkhorst HJ, Pack JD (1976) Special points for Brillouin-zone integrations. Physical Review B 13(12): 5188.

